19
Differential Chaos in Phase Space

In Chap. 18 on bugs, we discovered that a simple nonlinear difference *equation yields solutions that may be simple, complicated, or chaotic. In this chapter, we continue our study of nonlinear behavior, this time for two systems described by differential equations, the driven realistic pendulum, and coupled predator–prey populations. Because chaotic behavior may resemble noise, it is important to be confident that the unusual behaviors arise from physics and not numerics. Before we explore the solutions, we provide some theoretical background in the use of phase-space plots for revealing the beauty and simplicity underlying complicated behaviors. Our emphasis there is on using phase space as an example of the usefulness of an abstract space displaying the simplicity that often underlies complexity. Our study is based on the description in [35], on the analytic discussion of the* parametric oscillator *[31], and on a similar study of the vibrating pivot pendulum [17].*

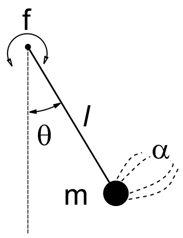

Fig. 19.1 A pendulum of length l driven through air by an external, sinusoidal torque. The strength of the torque is given by f and that of air resistance by α.

19.1
Problem: A Pendulum Becomes Chaotic (Differential Chaos)

Your **problem** is to describe the motion of this pendulum, first with the driving torque is turned off, but the initial velocity is large enough to send the pendulum over the top, and then when the driving torque is turned on. In Fig. 19.1, we see a pendulum of length l, *driven* by an external, sinusoidal torque **f** through air with a coefficient of drag α. Because there is no restriction that the angular displacement θ be small, we call this a *realistic* pendulum.

Computationyal Physics. Problem Solving with Computers (2nd edn).
Rubin H. Landau, Manuel José Páez, Cristian C. Bordeianu

ISBN: 978-3-527-40626-5

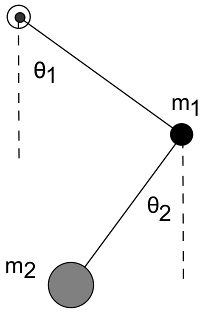

Fig. 19.2 A double pendulum.

Alternative Problem: For those of you who have already studied the realistic pendulum, study instead the double pendulum without any small-angle approximation (Fig. 19.2 and animation `DoublePend.mpg` on the CD). A double pendulum has a second pendulum connected to the first, and because each pendulum acts as a driving force to the other, we need not include a, external driving torque to produce a chaotic system (there are enough degrees of freedom without it).

19.2
Equation of Chaotic Pendulum

The theory of the *chaotic pendulum* is just that of a pendulum with friction and a driving torque (Fig. 19.1), but with no small-angle approximation. Newton's laws of rotational motion tell us that the sum of the gravitational torque $-mgl\sin\theta$, the frictional torque $-\beta\dot{\theta}$, and the external torque $\tau_0\cos\omega t$ equals the moment of inertia of the pendulum times its angular acceleration:

$$I\frac{d^2\theta}{dt^2} = -mgl\sin\theta - \beta\frac{d\theta}{dt} + \tau_0\cos\omega t \tag{19.1}$$

$$\Rightarrow \qquad \frac{d^2\theta}{dt^2} = -\omega_0^2\sin\theta \; - \alpha\frac{d\theta}{dt} + \; f\cos\omega t \tag{19.2}$$

where in (19.2) we obtain the traditional form with $\omega_0 = mgl/I$, $\alpha = \beta/I$, and $f = \tau_0/I$ [35]. Equation (19.2) is a second-order, time-dependent, nonlinear differential equation. The nonlinearity arises from the $\sin\theta$, as opposed to the θ, dependence of the gravitational torque. The parameter ω_0 is the natural frequency of the system arising from the restoring torque, α is a measure of the strength of friction, and f is a measure of the strength of the driving torque. In the standard ODE form, $d\mathbf{y}/dt = \mathbf{y}$ (Chap. 15), we have two simultaneous first-order equations:

$$\frac{dy^{(0)}}{dt} = y^{(1)} \qquad \frac{dy^{(1)}}{dt} = -\omega_0^2\sin y^{(0)} - \alpha y^{(1)} + f\cos\omega t \tag{19.3}$$

where $y^{(0)} = \theta(t)$ and $y^{(1)} = d\theta(t)/dt$

19.2.1 Oscillations of a Free Pendulum

If we ignore friction and external torques, (19.2) takes the simple form

$$\frac{d^2\theta}{dt^2} = -\omega_0^2 \sin\theta \tag{19.4}$$

If displacements are small, we can approximate $\sin\theta$ by θ and obtain the linear equation of simple harmonic motion with frequency ω_0:

$$\frac{d^2\theta}{dt^2} \simeq -\omega_0^2\theta \qquad \Rightarrow \qquad \theta(t) = \theta_0 \sin(\omega_0 t + \phi) \tag{19.5}$$

In Chap. 15, we have studied how nonlinearities produce anharmonic oscillations, and, indeed, (19.4) is another good candidate for such studies. As before, we expect solutions of (19.4) for the free realistic pendulum to be periodic, but with a frequency ω that equals $\omega_0 = 2\pi/T_0$, only for small oscillations. Furthermore, because the restoring torque $mgl\sin\theta \simeq mgl(\theta - \theta^3/3)$, is less than the $mgl\theta$ assumed in a harmonic oscillator, realistic pendulum swing slower (longer periods) as their angular displacements are made larger.

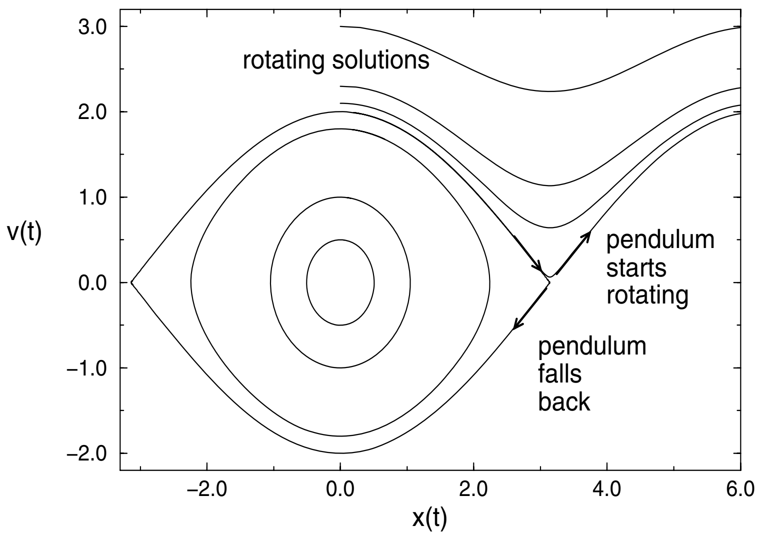

Fig. 19.3 Phase-space trajectories for a plane pendulum including "over the top" or rotating solutions. (Although not shown completely, the trajectories are symmetric with respect to vertical and horizontal reflections through the origin.)

19.2.2
Pendulum's "Solution" as Elliptic Integrals

The analytic solution to the realistic, free pendulum is a text book problem [23, 26,31]; except it is hardly a solution, and it is hardly analytic. The "solution" is based on energy being a constant (integral) of the motion. For simplicity, we start the pendulum off at rest from its maximum displacement θ_m. Because the initial energy is all potential, we know that the total energy of the system is its initial potential energy (Fig. 19.1),

$$E = PE(0) = mgl - mgl\cos\theta_m = 2mgl\sin^2(\theta_m/2) \tag{19.6}$$

Yet since $E = KE + PE$ is a constant, we can write for any value of θ

$$2mgl\sin^2\tfrac{\theta_m}{2} = \tfrac{1}{2}I(\,d\theta/dt)^2 + 2mgl\sin^2\tfrac{\theta}{2}$$

$$\Rightarrow\quad \frac{d\theta}{dt} = 2\omega_0\left[\sin^2\tfrac{\theta_m}{2} - \sin^2\tfrac{\theta}{2}\right]^{1/2} \Rightarrow\quad \frac{dt}{d\theta} = \frac{T_0/\pi}{\left[\sin^2\tfrac{\theta_m}{2} - \sin^2\tfrac{\theta}{2}\right]^{1/2}}$$

$$\Rightarrow\quad \frac{T}{4} = \frac{T_0}{4\pi}\int_0^{\theta_m}\frac{d\theta}{\left[\sin^2\tfrac{\theta_m}{2} - \sin^2\tfrac{\theta}{2}\right]^{1/2}} = \frac{T_0}{4\pi\sin\theta_m}F(\tfrac{\theta_m}{2},\tfrac{\theta}{2}) \tag{19.7}$$

$$\Rightarrow\quad T \simeq T_0\left[1 + \tfrac{1}{4}\sin^2\tfrac{\theta_m}{2} + \tfrac{9}{64}\sin^4\tfrac{\theta_m}{2} + \cdots\right] \tag{19.8}$$

where we have assumed that it takes $T/4$ for the pendulum to travel from $\theta = 0$ to θ_m. The integral in (19.7) is an *elliptic integral of the first kind*. If you think of an elliptic integral as a generalization of a trigonometric function, then this is a closed-form solution; otherwise it's an integral needing computation. The series expansion (19.8) is obtained by expanding the denominator and integrating term by term. It tells us, for example, that an amplitude of 80^o leads to a 10% slowdown of the pendulum. In contrast, we will determine the period empirically by solving for $\theta(t)$ and counting times between one $\theta = 0$ to the next.

19.2.3
Implementation and Test: Free Pendulum

As a preliminary to the solution of the full equation (19.2), modify your `rk4` program to solve (19.4) for the free oscillations of a realistic pendulum.

1. Start your pendulum off at $\theta = 0$ with $\dot\theta(0) \neq 0$. Gradually increase $\dot\theta(0)$ to increase the importance of nonlinearlities.

2. Test your program for the linear case ($\sin\theta \to \theta$), verify that

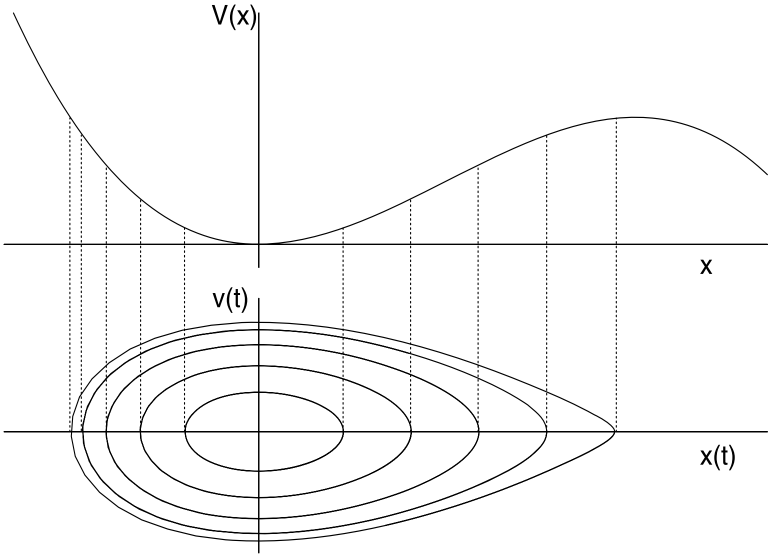

Fig. 19.4 A potential-energy plot for a nonharmonic oscillator (top) and a phase-space plot (lower) for the same nonharmonic oscillator. Note that the ellipse-like figures are neither ellipses nor symmetric with respect to the v axis. The different orbits correspond to different energies, as indicated by the limits within the potentials.

(a) your solution is harmonic with frequency $\omega_0 = 2\pi/T_0$, and

(b) the frequency of oscillation is independent of the amplitude.

3. Devise an algorithm to determine the period T of the oscillation by counting the time it takes for four successive passes of the amplitude through $\theta = 0$. (You need *four* passes because a general oscillation may not be symmetric about the origin.) Test your algorithm for simple harmonic motion where you know T_0.

4. For the realistic pendulum, observe the change in period as a function of increasing initial energy or displacement. Plot your observations along with (19.8).

5. Verify that as the initial KE approaches $2mgl$, the motion remains oscillatory, but not harmonic.

6. At $E = 2mgl$ (the *separatrix*), the motion changes from oscillatory to rotational ("over the top" or "running"). See how close you can get to the separatrix and try to verify that at precisely this energy it takes an infinite time for a single oscillation.

19.3 Visualization: Phase-Space Orbits

The conventional solution to an equation of motion is the position $x(t)$ and the velocity $v(t)$ as functions of time. Often, behaviors that appear complicated as functions of time, appear simpler when viewed in an abstract space called *phase space*, where the ordinate is the velocity $v(t)$ and the abscissa is the position $x(t)$ (Figs. 19.5 and 19.4). As we see from the figures, when viewed in phase space, solutions of the equations of motion form geometric objects that are easy to recognize.

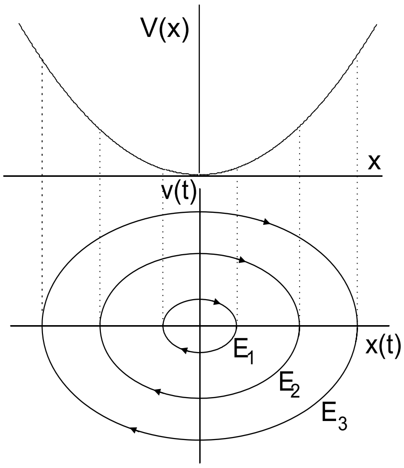

Fig. 19.5 A phase-space plot of velocity versus position for a harmonic oscillator. Because the ellipses close, the system must be periodic. The different orbits correspond to different energies, as indicated by the limits within the potentials.

The position and velocity of a free harmonic oscillator are given by the trigonometric functions:

$$x(t) = A\sin(\omega t) \qquad v(t) = \frac{dx}{dt} = \omega A\cos(\omega t) \tag{19.9}$$

When substituted into the total energy, we obtain two important results:

$$E = KE + PE = (\tfrac{1}{2}m)\, v^2 + (\tfrac{1}{2}\omega^2 m^2)\, x^2 \tag{19.10}$$

$$= \frac{\omega^2 m^2 A^2}{2m}\cos^2(\omega t) + \tfrac{1}{2}\omega^2 m^2 A^2 \sin^2(\omega t) = \tfrac{1}{2}m\omega^2 A^2 \tag{19.11}$$

The first equation, being that of an ellipse, proves that the harmonic oscillator follows closed elliptical orbits in phase space, with the size of the ellipse increasing with the system's energy. The second equation proves that the total energy is a constant of the motion. Different initial conditions having the

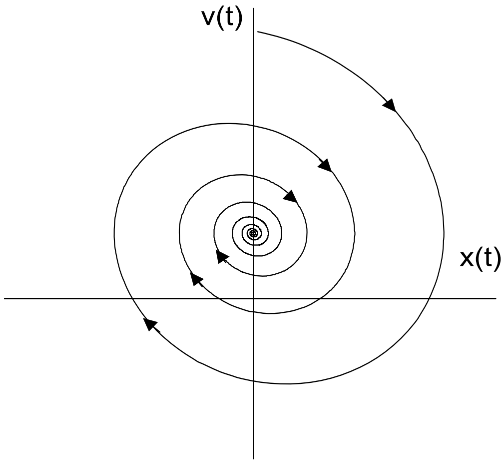

Fig. 19.6 Phase-space trajectories for a particle in a repulsive potential. Notice the absence of trajectories in the regions forbidden by energy conservation.

same energy start at different places on the same ellipse, but transverse the same orbits.

In Figs. 19.3–19.8, we show some typical phase-space structures. *Study these figures and their captions*, and note the following:

- For anharmonic oscillations, the orbits will still be ellipse like, but with angular corners that become more distinct with increasing nonlinearity.

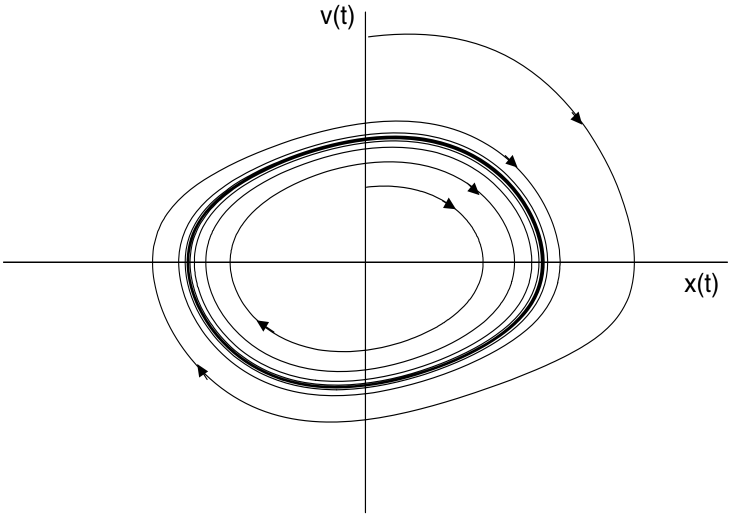

Fig. 19.7 A phase-space orbit for an oscillator with friction. The system eventually comes to rest at the origin.

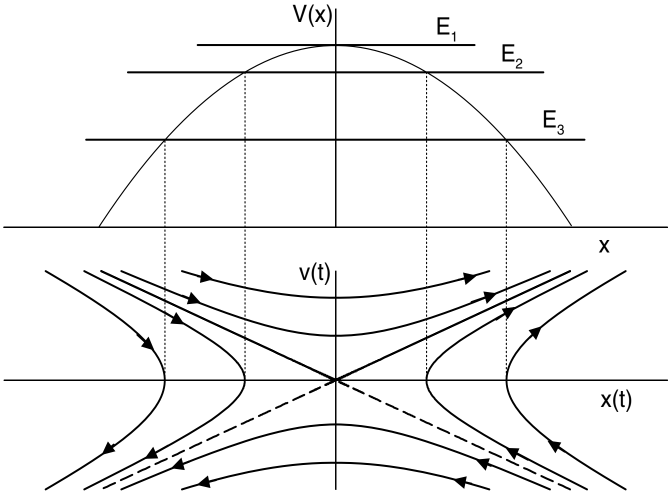

Fig. 19.8 Two phase-space trajectories corresponding to solutions of the van der Pol equation. One trajectory approaches the limit cycle (the dark curve) from the inside, while the other approaches it from the outside.

- Closed trajectories describe periodic oscillations (the same (x, v) occur again and again), with clockwise motion.
- Open orbits correspond to nonperiodic or "running" motion (a pendulum rotating like a propeller).
- Regions of space where the potential is repulsive, lead to open trajectories in phase space (Fig. 19.8).
- As seen in Fig. 19.3, the separatrix corresponds to the trajectory in phase space that separates open and closed orbits. Motion on the separatrix is indeterminant as the pendulum may balance at the maxima of $V(\theta)$.
- Friction may cause the energy to decrease with time and the phase-space orbit to spiral into a *fixed point* (Fig. 19.6).
- For certain parameters, a closed *limit cycle* (Fig. 19.8) occurs in which the energy pumped in by the external torque exactly balances that lost by friction.
- Because solutions for different initial conditions are unique, different orbits do not cross. Nonetheless, open orbits do come together at the points of unstable equilibrium (*hyperbolic points* in Figs. 19.8 and 19.3), where an indeterminacy exists.

19.3.1 Chaos in Phase Space

It is easy to solve the nonlinear ODE (19.3) on the computer. It is not so easy, however, to understand the solutions because they are so rich (*alias* for complex and highly sensitive to initial conditions). The solutions are easier to understand in phase space, and particularly if you learn to recognize some characteristic structures there. Actually, there are a number of "tools" that can be used to decide if a system is chaotic, in contrast to just complex. Phase-space structures is one of them, and determination the Lyupanov coefficient [3], is another. What is important is being able to deduce the simplicity that lies within the complicated behavior.

What is surprising is that even though the ellipse-like figures we have been discussing were deduced for free systems with no friction and no driving torque, similar structures continue to exist for driven systems with friction. The trajectories may not remain on a single structure for all times, but they are *attracted* to them. In contrast to periodic motion, which corresponds to closed figures in phase space, random motion appears as a diffuse cloud filling an entire energetically accessible region. Complex, or chaotic motion falls someplace in between (Fig. 19.9). If viewed for long times and many initial conditions, chaotic flows through phase space, while resembling the familiar geometric figures, may contain dark or diffuse *bands* in places rather than single lines. The continuity of trajectories within bands means that there is a continuum of solutions possible, and that the system flows continuously among the different trajectories forming the band. The transitions among solutions is what causes the coordinate space solutions to appear chaotic, and is what makes them hypersentive to initial conditions (the slightest change in which causes the system to flow to nearby trajectories).

So even though the motion may be chaotic, the definite shapes of the phase-space structures means that there is a well-defined and simple underlying order within chaos. Pick out the following phase-space structures in your simulations:

Limit cycles. When the chaotic pendulum is driven by a not-too-large driving torque, it is possible to pick the magnitude for this torque such that after the initial transients die off, the average energy put into the system during one period exactly balances the average energy dissipated by friction during that period (Fig. 19.8):

$$\langle f \cos\omega t \rangle = \left\langle \alpha \frac{d\theta}{dt} \right\rangle = \left\langle \alpha \frac{d\theta}{dt}(0) \cos\omega t \right\rangle \qquad \Rightarrow \qquad f = \alpha \frac{d\theta}{dt}(0) \quad (19.12)$$

This leads to *limit cycles*, which appear as closed ellipse-like figures, even in the presence of friction and driving torque. Yet the solution may be unstable and make sporadic jumps between limit cycles.

Predictable attractors. Well-defined, fairly simple periodic behaviors that are not particularly sensitive to initial conditions. These are orbits, such as fixed points and limit cycles, into which the system settles. If your location in phase space is near a predictable attractor, ensuing times will bring you to it.

Strange attractors: Well-defined, yet complicated, semiperiodic behaviors that appear to be uncorrelated to the motion at an earlier time. They are distinguished from predicable attractors by being fractal (Chap. 20), chaotic, and highly sensitive to initial conditions [22]. Even after millions of oscillations, the motion remains *attracted* to them.

Chaotic paths: Regions of phase space that appear as filled-in bands rather than lines. Continuity within the bands implies complicated behaviors, yet still with simple underlying structure.

Mode locking: When the magnitude f of the driving torque is larger than that for a limit cycle, (19.12), the driving torque overpowers the natural oscillations, and the steady-state motion is at the frequency of the driver. This is *mode locking*. While mode locking can occur for linear or nonlinear systems, for nonlinear systems the driving torque may lock onto the system by exciting its overtones, leading to a rational relation between driving frequency and natural frequency:

$$\frac{\omega}{\omega_0} = \frac{n}{m} \qquad n, m = \text{ integers} \tag{19.13}$$

Butterfly effects: One of the classic quips about the hypersensitivity of chaotic systems to initial conditions is that the weather pattern in North America is hard to predict well because it is sensitive to the flapping of butterfly wings in South America. Although this appears to be counter intuitive because we know that systems with essentially identical initial conditions should behave the same, eventually the systems diverge.

19.3.2
Assessment in Phase Space

The challenge with simulations of the chaotic pendulum (19.3) is that the 4D parameter space $(\omega_0, \alpha, f, \omega)$ is immense. For normal behavior, sweeping through ω should show resonances and beating; sweeping through α should show underdamping, critical damping, and overdamping; sweeping through f should show mode locking (for the right values of ω). All these behaviors can be found in the solution of your differential equation, yet because they get mixed together, your solution may exhibit quite complex behavior.

In this assessment you should try to reproduce the behaviors shown in the phase-space diagrams of Fig. 19.9. Beware*, because the system is chaotic, your results may be very sensitive to the exact values of the initial conditions, or to the precision of your integration routine. We suggest that you experiment; start with the parameter*

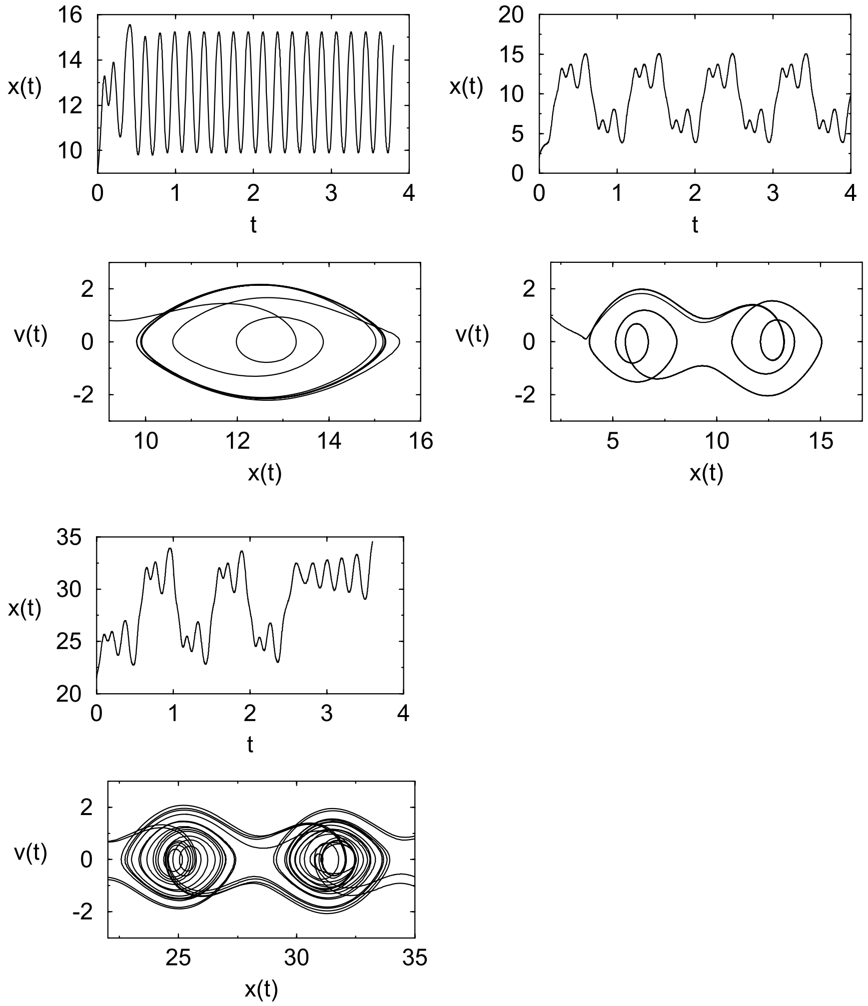

Fig. 19.9 Position and phase-space plots for the chaotic pendulum with $\omega_0 = 1$, $\alpha = 0.2$, $f = 0.52$, and $\omega = 0.666$. The angular position is $x(t)$ and the angular velocity is $v(t)$. The chaotic regions are the dark bands in the bottom figure.

values we used to produce our plots, and then observe the effects of making very small *changes in parameter until you obtain different modes of behavior. Absence of agreement with our exact values does not imply that anything is "wrong."*

1. Take your solution to the realistic pendulum ($\sin\theta$), and include friction, making α an input parameter. Run for a variety of initial conditions, including over-the-top ones; you should see spirals like those in Figs. 19.7 and 19.8.

2. Next, verify that with no friction, but with a very small driving torque, you obtain a perturbed ellipse.

3. Set driving torque's frequency to be close to the natural frequency ω_0 of the pendulum, and produce beats. Note that you may need to adjust the magnitude and phase of the driving torque to avoid an "impedance mismatch" between the pendulum and driver.

4. Finally, include friction and a variable-frequency driving torque. Scan ω to produce a nonlinear resonance (which looks like beating).

5. **Explore chaos:** Start off with the initial conditions we used in Fig. 19.9,

$$(x_0, v_0) = (-0.0885, 0.8) \qquad (-0.0883, 0.8) \qquad (-0.0888, 0.8)$$

   To save time and storage, you may want to use a larger time step for plotting than that used to solve the differential equations.

6. Indicate which parts of the plots correspond to transients.

7. Ensure that you have found
   (a) a period-three limit cycle where the pendulum jumps between three major orbits in phase space;
   (b) a running solution where the pendulum keeps going over the top;
   (c) chaotic motion in which some paths in phase space appear as bands.

8. Look for the "butterfly effect." Start two pendulums off with identical positions, but velocities that differ by one part in a thousand. Notice how the initial motion is essentially identical, but how at some later time the motions diverge.

19.4 Assessment: Fourier Analysis of Chaos

We have seen that a realistic pendulum feels a restoring torque, $\tau_g \propto \sin\theta \simeq \theta - \theta^3/3! + \theta^5/5! + \cdots$, that contains nonlinear terms which lead to nonharmonic behavior. In addition, when a realistic pendulum is driven by an external sinusoidal torque, the pendulum may mode lock with the driver and so oscillate at a frequency that is rationally related to the driver's. Consequently, the behavior of the realistic pendulum is expected to be a combination of various periodic behaviors, with discrete jumps between different modes.

In this assessment you should determine the Fourier components present in the pendulum's complicated and chaotic behaviors. You should show that a three-cycle structure, for example, contains three major Fourier components, while a five-cycle has five. You should also notice that when the pendulum goes over the top, its spectrum contains a steady-state ("dc") component.

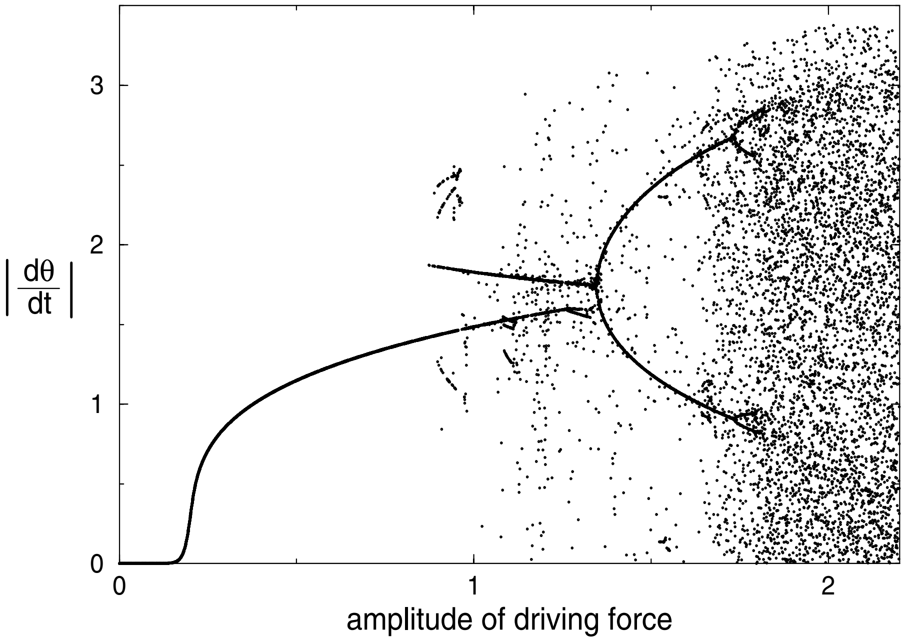

Fig. 19.10 Bifurcation diagram for the damped pendulum with a vibrating pivot. The ordinate is $|d\theta/dt|$, the absolute value of the instantaneous angular velocity at the beginning of the period of the driver, and the abscissa is the magnitude of the driving force d. Note that the heavy line results from overlapping of points, not from connecting the points.

1. Dust off your program which analyzes a $y(t)$ into Fourier components. Alternatively, you may use a Fourier analysis tool contained in your graphics program or system library (e.g., Grace and OpenDX).

2. Apply your analyzer to the solution of the chaotic pendulum for the cases where there are one-, three-, and five-cycle structures in phase space. Deduce the major frequencies contained in these structures.

3. Try to deduce a relation between the Fourier components, the natural frequency ω_0, and the driving frequency ω.

4. A classic signal of chaos is a broadband, although not necessarily flat, Fourier spectrum. Examine your system for parameters that give chaotic behavior and verify this statement.

19.5 Exploration: Bifurcations in Chaotic Pendulum

We have already stated that a chaotic system contains a finite number of dominant frequencies that occur sequentially, in contrast to linear systems where they occur simultaneously. Consequently, if we sample the instantaneous angular velocity $\dot{\theta} = d\theta/dt$ of a chaotic system at various instances of time, we should get different values each time, but with the major Fourier components occurring more often than others.[1] These are the frequencies to which the system is *attracted*. Yet if we change some parameter of the system, then we expect the dominant components to change, with some new ones entering, and some old ones departing. That being the case, if we make a scatter plot of the frequencies sampled for all times at one particular value of the driving force, and then change the magnitude of the driving force slightly and sample frequencies again, the resulting plot should show distinctive patterns of frequencies. That a bifurcation diagram is obtained by making such a plot, and that it is similar to the bifurcation diagram for bug populations studied in Unit I, is one of the mysteries of life.

In the scatter plot in Fig. 19.10, we sampled $\dot{\theta}$ for the motion of a chaotic pendulum with a vibrating pivot point (in contrast to our usual vibrating external torque). This pendulum is similar to our chaotic one (19.2), but with the driving force depending on $\sin\theta$:

$$\frac{d^2\theta}{dt^2} = -\alpha\frac{d\theta}{dt} - \left(\omega_0^2 + f\cos\omega t\right)\sin\theta \tag{19.14}$$

Essentially, the acceleration of the pivot is equivalent to a sinusoidal variation of g or ω_0^2. Analytic [31, Sections 25–30] and numeric [17, 38] studies of this system exist.

We leave it to you to produce a bifurcation diagram from your chaotic pendulum with the same technique. We obtained the bifurcation diagram (Fig. 19.10) by following these steps (a modification of those in [38]):

1. Use the initial conditions: $\theta(0) = 1$ and $\dot{\theta}(0) = 1$.
2. Set $\alpha = 0.1$, $\omega_0 = 1$, $\omega = 2$, and let f vary through the range in Fig. 19.10.
3. For each value of f, wait 150 periods of the driver before sampling to permit transients to die off. Sample the instantaneous angular velocity $\dot{\theta}$ for 150 times whenever the driving force passes through $\theta = 0$.
4. Plot the 150 values of $|\dot{\theta}|$ versus f.
5. Repeat the procedure for each new value of f.

[1] We refer to this angular velocity as $\dot{\theta}$ since we have already used ω for the frequency of the driver and ω_0 for the natural frequency.

19.6 Exploration: Another Type of Phase-Space Plot

Imagine that you have measured the displacement of some system as a function of time. Your measurements appear to indicate characteristic nonlinear behaviors, and you would like to check this by making a phase-space plot, but without going to the trouble of measuring the conjugate momenta to plot versus displacement. Amazingly enough, one may also plot $x(t+\tau)$ versus $x(t)$ as a function of time to obtain a phase-space plot [39]. Here τ is a *lag time* that should be chosen as some fraction of a characteristic time for the system under study. While this may not seem like a valid way to make a phase-space plot, recall the forward-difference approximation for the derivative,

$$v(t) = \frac{dx(t)}{dt} \simeq \frac{x(t+\tau) - x(t)}{\tau} \tag{19.15}$$

We see that plotting $x(t+\tau)$ vs. $x(t)$ is equivalent to plotting $v(t)$ vs. $x(t)$.

Exercise: Create a phase-space plot from the output of your chaotic pendulum by plotting $\theta(t+\tau)$ versus $\theta(t)$ for a large range of t values. Explore how the graphs change for different values of the lag time τ. Compare your results to the conventional phase-space plots you obtained previously.

19.7 Further Explorations

1. The nonlinear behavior in once-common objects such as vacuum tubes and metronomes are described by the **van der Pool equation**,:

   $$\frac{d^2x}{dt^2} + \mu(x^2 - x_0^2)\frac{dx}{dt} + \omega_0^2 x = 0 \tag{19.16}$$

   The behavior predicted for these systems is *self-limiting* because the equation contains a limit cycle that is also a predictable attractor. You can think of (19.16) as describing an oscillator with x-dependent damping (the μ term). If $x > x_0$, friction slows the system down; if $x < x_0$, friction speeds the system up. A resulting phase-space orbit is similar to that shown in Fig. 19.8. The heavy curve is the *limit cycle*. Orbits internal to the limit cycle spiral out until they reach the limit cycle; orbit external to it spiral in.

2. **Duffing oscillator:** Another damped and driven nonlinear oscillator is

   $$\frac{d^2\theta}{dt^2} - \tfrac{1}{2}\theta(1-\theta^2) = -\alpha\frac{d\theta}{dt} + f\cos\omega t \tag{19.17}$$

While similar to the chaotic pendulum, it is easier to find multiple attractors with this oscillator [40].

3. **Lorenz attractor:** In 1962 Lorenz [24] was looking for a simple model for weather prediction, and simplified the heat-transport equations to

$$\frac{dx}{dt} = 10(y - x) \qquad \frac{dy}{dt} = -xz + 28x - y \qquad \frac{dz}{dt} = xy - \tfrac{8}{3}z \quad (19.18)$$

The solution of these simple nonlinear equations gave the complicated behavior that has led to the modern interest in chaos (after considerable doubt regarding the reliability of the numerical solutions).

4. **A 3D computer fly:** Plot, in 3D space, the equations

$$x = \sin ay - z \cos bx \qquad y = z \sin cx - \cos dy \qquad z = e \sin x \quad (19.19)$$

Here the parameter e controls the degree of apparent randomness.

5. **Hénon-Heiles potential:** The potential and Hamiltonian

$$V(x, y) = \tfrac{1}{2}x^2 + \tfrac{1}{2}y^2 + x^2 y - \tfrac{1}{3}y^3 \qquad H = \tfrac{1}{2}p_x^2 + \tfrac{1}{2}p_y^2 + V(x, y) \quad (19.20)$$

are used to describe three astronomical objects interacting. They bind the objects near the origin, but release them if they move far out. The equations of motion for this problem follow from the Hamiltonian equations:

$$\frac{dp_x}{dt} = -x - 2xy \qquad \frac{dp_y}{dt} = -y - x^2 + y^2 \qquad \frac{dx}{dt} = p_x \qquad \frac{dy}{dt} = p_y$$

(a) Numerically solve for the position $[x(t), y(t)]$ for a particle in the Hénon-Heiles potential.

(b) Plot $[x(t), y(t)]$ for a number of initial conditions. Check that the initial condition $E < 1/6$ leads to a bounded orbit.

(c) Produce a Poincaré section in the (y, p_y) plane by plotting (y, p_y) each time an orbit passes through $x = 0$.